

RAPID FORMATION OF FRAMBOIDAL SULFIDES ON BONE SURFACES FROM A SIMULATED MARINE CARCASS FALL

Author(s): LAURA A. VIETTI, JAKE V. BAILEY, DAVID L. FOX, and RAYMOND R. ROGERS

Source: PALAIOS, 30(4):327-334.

Published By: Society for Sedimentary Geology

URL: <http://www.bioone.org/doi/full/10.2110/palo.2014.027>

BioOne (www.bioone.org) is a nonprofit, online aggregation of core research in the biological, ecological, and environmental sciences. BioOne provides a sustainable online platform for over 170 journals and books published by nonprofit societies, associations, museums, institutions, and presses.

Your use of this PDF, the BioOne Web site, and all posted and associated content indicates your acceptance of BioOne's Terms of Use, available at www.bioone.org/page/terms_of_use.

Usage of BioOne content is strictly limited to personal, educational, and non-commercial use. Commercial inquiries or rights and permissions requests should be directed to the individual publisher as copyright holder.

RAPID FORMATION OF FRAMBOIDAL SULFIDES ON BONE SURFACES FROM A SIMULATED MARINE CARCASS FALL

LAURA A. VIETTI,^{1,2} JAKE V. BAILEY,¹ DAVID L. FOX,¹ AND RAYMOND R. ROGERS³

¹University of Minnesota, Department of Earth Sciences, Minneapolis, Minnesota, 55455, USA

²Current address: University of Wyoming, Department of Geology and Geophysics, Laramie, Wyoming, USA

³Macalester College, Geology Department, Saint Paul, Minnesota, 55105, USA

e-mail: Lvietti@uwyo.edu

ABSTRACT: Sulfide mineral framboids associated with fossil bones in marine settings may aid in taphonomic reconstructions because framboids reflect the geochemical conditions under which they form. However, the timing and mechanism(s) of framboid formation on bone remain poorly understood. To better constrain the initial formation of framboids during decomposition of bone in marine depositional environments, we simulated aspects of bone decay on the ocean floor and analyzed framboids found on bone surfaces and in the associated sediment. We observed that framboids formed on bone surfaces within one week of experimentation, and were associated with reducing conditions within a dark-colored microbial mat overlain by oxic waters. Statistical and discriminant analyses of elemental data show that bone-hosted framboids formed *in situ* on the bone surfaces. Close associations of framboids with sulfidic microbial biofilms indicate that bone-hosted framboids resulted from conditions generated during the microbial degradation of bone-associated organic matter. Our results suggest that framboids can form on bone surfaces while bones rest on the seafloor prior to burial and perhaps prior to the so-called sulphophilic stage of whale-fall animal colonization. We compared experimentally produced framboids with published sedimentary framboid populations. Bone-hosted framboids resemble smaller and less variably sized sedimentary framboid populations canonically known to form in anoxic water columns, even though the bone-hosted framboids were overlain by oxygenated conditions. We propose that the period available for framboid growth is shorter on bone surfaces than in sediments, because geochemical conditions that favor sulfide mineral precipitation on bone are transient. Shorter growing periods and localized conditions result in smaller framboid sizes that may not reflect ambient conditions in a water column.

INTRODUCTION

Framboids are spherical mineral aggregates composed of densely packed microcrystals that most commonly occur as pyrite and occasionally as other sulfides (Love 1967; Canfield and Raiswell 1991). Framboids have been found in association with fossil material from marine environments including fossil plant material (Allison 1988; Canfield and Raiswell 1991), fossil sponge spicules (Zhou and Jiang 2009), and a variety of marine vertebrate material including Mesozoic marine reptile remains (Martill 1987; Kaim et al. 2008) and Cenozoic marine mammals (Naganuma et al. 1996; Amano and Little 2005; Amano et al. 2007; Shapiro and Spangler 2009).

Sulfidic framboids are well studied. Results from theoretical models, in conjunction with lab experiments and natural observations, provide constraints on the geochemical conditions favoring framboid growth in anoxic environments with high rates of sulfide diffusion and available reduced iron (Berner 1969, 1970; Farrand 1970; Sweeney and Kaplan 1973; Raiswell 1982). Although no single model for framboid growth is universally accepted, framboids are generally thought to form via several steps starting with the reaction of sulfide with detrital iron minerals (ferric hydroxide, goethite) or dissolved iron to form iron monosulfides (mackinawite), which in turn react with sulfur to nucleate framboids in anoxic environments (Love 1967; Raiswell 1982; Brett and Baird 1986). Raiswell (1982), Canfield and Raiswell (1991), Raiswell et al. (1993), and Ohfuji and Rickard (2005) provide detailed reviews of framboid growth.

Framboidal sulfides associated with fossil material in marine environments are commonly used as indicators of early diagenesis. For example, Brett and Baird (1986) compared crystal habits and textures of pyrite associated with fossil remains and suggested that framboidal pyrite found in association with fossil material is indicative of early diagenesis in shallowly buried sediments, whereas euhedral pyrite may indicate later diagenesis of the organic material at greater depths in the sediment. Framboid formation in sediments during early diagenesis is attributed to the bacterial decay of organic matter, primarily by dissimilatory sulfate-reducing bacteria (SRBs) that produce sulfide via their anaerobic metabolisms (Raiswell et al. 1993). Similarly, previous studies suggest that the bacterial degradation of decaying organic matter prior to fossilization is also a source of framboids associated with fossils from marine environments (Allison 1988; Canfield and Raiswell 1991; Grimes et al. 2002). However, it is unclear at what stage during early diagenesis framboids are likely to form on marine vertebrate fossils.

Early diagenesis typically refers to processes that affect skeletal material prior to deep burial (i.e., > 5 m), which would include decay, alteration, and permineralization on the ocean floor and also processes in shallow-burial environments. Early diagenesis may encompass a period as short as 10 years (Lundsten et al. 2010) to over thousands of years, as postulated for some marine bone beds (Pyenson et al. 2009). During early diagenesis, Amano and Little (2005) correlated the appearance of framboids to the sulphophilic decay stage where sulfate-reducing bacteria, exploiting exposed bone on the seafloor, produce steep

TABLE 1.—Mean and standard deviation for characteristics measured from framboid populations associated with bone and sediment. Gray boxes indicate statistically significant differences ($p < 0.05$) between the bone-hosted and sediment-hosted framboid populations.

Population type	Week sampled	n	Framboid diameter (μm)	Microcrystal diameter (μm)	Atom % Fe	Atom % S	Atom % C	Fe:S
Bone total	1–3	59	3.9 \pm 1.1	0.7 \pm 0.3	7.9 \pm 3.0	10.6 \pm 5.8	47.0 \pm 16.6	1.3 \pm 1.7
Sediment total	0–3	36	4.3 \pm 1.7	0.8 \pm 0.4	3.3 \pm 1.2	5.5 \pm 1.8	34.2 \pm 11.2	0.6 \pm 0.3

oxygen-sulfide gradient conditions that supports a sulfide-dependent ecosystem that can develop beginning \sim 2–50 years after death in recent carcass falls (Smith and Baco 2003). Conversely, other researchers suggest that framboids form during shallow burial when bones enter into sulfide-enriched zones in the sediment. To date, there are few reported examples of pyrite forming on modern ($<$ 10,000 years old) vertebrate remains (Turner-Walker and Jans 2008; Hollund et al. 2012; Turner-Walker 2012), and even fewer from modern marine environments (Kasuya and Ando 2005).

Although framboids are commonly used indicators of early burial conditions related to microbial sulfide production, the specific timing of framboid formation on bone surfaces is not clear. Here, we present laboratory observations of framboid formation on bone surfaces from lab-simulated carcass falls, and provide new insights into the significance and initial timing of sulfidic framboids found associated with vertebrate fossil material in marine environments. The restricted scope of our study precludes us from placing constraints on other types of framboid formation, although it is likely that the geochemical window permitting framboid formation extends past the duration of our experiment.

METHODS

Experimental Design

Lab-simulated carcass falls were used to study the formation of framboidal sulfides on bone surfaces associated with natural carcass falls (sunken vertebrate remains on the ocean floor). Simulated carcass falls were created by adding 50 ml of naturally inoculated marine mud and 200 ml of natural seawater to a 300 ml lidded plastic container. Sediment and seawater were collected from the coast of Massachusetts (N 41°42'0", W 70°45'1", 1 m water depth). The elemental composition of the marine sediment from the site of collection is provided in Supplementary Data¹ Table S1. The concentration of primary cations and anions of the seawater from the collection site are reported in Supplementary Data Tables 2 and 3. Mesocosms were incubated in near-dark conditions at 10°C for two weeks to establish stable conditions for sediment-hosted microbial communities. After two weeks, two defleshed domestic pig rib sections (\sim 1 cm³) were emplaced on the sediment/water interface in each mesocosm. Syringe tips connected to an aquarium air pump were extended \sim 1 cm into the water column to aerate the water and better simulate open-ocean circulation.

Three separate carcass-fall simulations and one control mesocosm were made, and framboid populations were sampled from the sediment of each carcass-fall simulation prior to bone emplacement to control for preexisting framboid populations. After bone emplacement, a different mesocosm was sampled each week for three weeks; sampling a separate mesocosm was done to avoid disturbing any biofilms or resuspending sediment during sampling. At each sampling period, oxygen profiles were measured, biofilm and sediment samples were collected, and photographs were taken of the sampled carcass-fall mesocosm. To document the correlation of sediment-hosted microbial life and framboid growth on bone, we included a control composed of sterilized seawater and sediment.

Analytical Methods

To measure microbial oxygen consumption, oxygen profiles were measured in the carcass-fall mesocosm at each sampling interval using Clark-type amperometric oxygen sensors attached to a micromanipulator (Revsbech and Jørgensen 1986; Revsbech 1989; Unisense, Aarhus, Science Park Aarhus, Denmark). Prior to measuring, the microsensor was depolarized and calibrated. Profiles started \sim 1.5 cm above the sediment/water interface, extended through the biofilm directly adjacent to the bone, and extended \sim 1 cm into the sediment. Due to vertical limitations of the micromanipulator, profiles extending from the water/air interface through the sediment were not possible to measure. Measurements were taken at 0.05 cm intervals and were reported as oxygen micromolar concentrations (μM).

Framboids observed on the surfaces of bone exposed to the water column, in addition to sediment-hosted framboids, were examined during each sampling period using a low-vacuum Hitachi TM-1000 SEM housed at LacCore (National Lacustrine Core Facility, University of Minnesota–Twin Cities); samples were uncoated and backscattered electron imaging was used to image specimens. Framboids were initially identified by their shape and high contrast compared to surrounding bone, biofilm, and sediment. Elemental abundances of iron, sulfur, and carbon were measured using an EDAX energy-dispersive X-ray spectrometer (EDS) running Bruker Quantax 50 software. The EDS was calibrated using copper because its K α X-ray energy does not overlap with the K α energy distribution of iron, sulfur, and carbon. Observations were made at an accelerating voltage of 15 kV, with acquisition times of 90 seconds. Relative, corrected, and atomic counts of detectable elements were reported. Framboid diameters were measured directly on the SEM image capture.

In addition to framboid diameter, semiquantitative measurements were also collected for atom % Fe, atom % S, and atom % C, microcrystal diameter, and Fe:S ratio. Sediment and bone-associated framboid populations were found to be statistically different based on MANOVA results, and observations were further compared using ANOVA with a *post hoc* all pairs comparison Tukey-Kramer test ($\alpha = 0.05$) for multiple group comparisons, and a Student's t-test for pairwise comparisons. Because multiple variables were reported per observation, discriminant analyses were performed to test group membership based on a multivariate approach. Groups were cross-validated to assess if the discriminant function had any predictive ability on data that was not used to build the function.

Results

Framboids were observed on bone surfaces from the carcass-fall simulations as early as the first week of experimentation and were observed through the third week when the experiment ended. Table 1 shows summary statistics for the framboid populations, and Figure 1 illustrates representative images of framboids on bone surfaces. Mean framboid diameter for all framboids observed on bones surfaces throughout the three-week experiment was 3.9 \pm 1.1 μm (SD) ($n = 59$), and the mean microcrystal size was 0.7 \pm 0.3 μm (SD) ($n = 57$). The medians and standard deviations of elemental data for the bone-

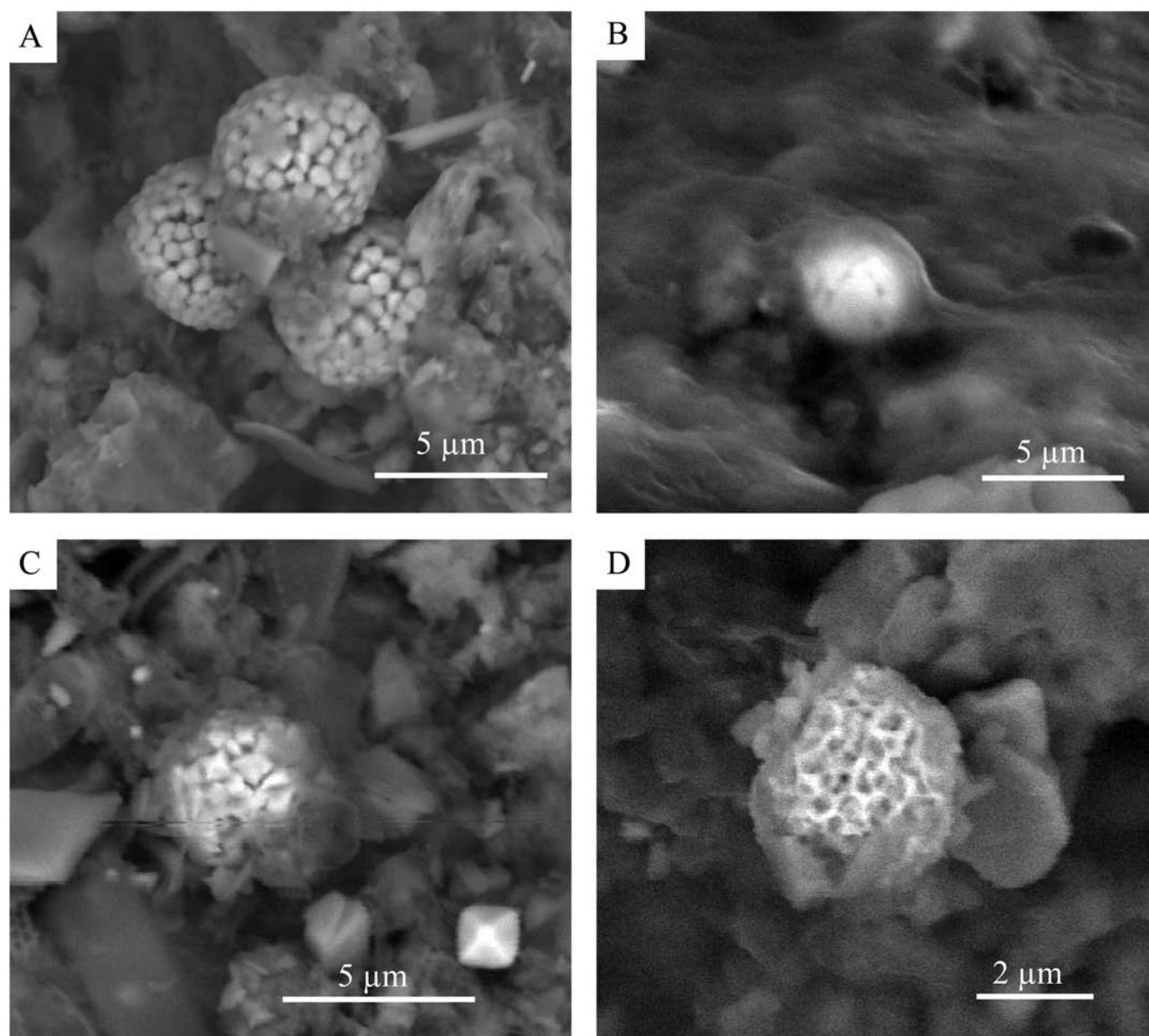


FIG. 1.—Backscattered electron SEM images of frambooids found on bone surfaces from carcass-fall experiments. **A)** Typical frambooid morphology observed on bones. **B)** Frambooid from the microbial mat surface encapsulated in probable extracellular polymeric substances. **C)** Frambooid with octahedral crystallites, also associated with putative biofilm. **D)** Example of frambooid with anhedral crystallites, thought to be a protoframbooid, also associated with putative biofilm.

associated frambooids were: atom % Fe = $7.9 \pm 3.0\%$, atom % S = $10.6 \pm 5.8\%$, and atom % C = $47.0 \pm 16.6\%$. The median Fe:S ratio for the bone-hosted frambooid population was 1.3 ± 1.7 . In addition to the frambooids, sulfide clusters, which are frambooid-like but do not have consistently shaped, sized, or ordered microcrystals (Canfield and Raiswell 1991; Ohfuji and Rickard 2005), were also observed on bone surfaces ($n = 4$). These sulfide clusters were found to be statistically similar in size and elemental composition to the bone-hosted frambooid populations (p -values > 0.3); although the sample size is likely too low to detect differences between frambooids and clusters. Raw data for bone-derived frambooids and clusters is shown in Supplementary Data Table 4. No frambooids were observed on bone surfaces from the sterilized control at any point during the experiment.

As frambooids were found in the sediment prior to bone placement, frambooids were also characterized from the sediment before and after bone deployment to distinguish preexisting sediment frambooids from newly formed frambooids. To do this, we tested whether the sediment and bone frambooid populations were statistically similar (null hypothesis) using MANOVA and Student's t -test, $\alpha = 0.05$. MANOVA results indicated the sediment and bone-associated frambooid populations are different ($F = 3.1$, $df = 6$, p -value < 0.0001). The Student's t -test results are summarized in Table 1 and raw data are included in Supplementary Data¹ Table S4. Sediment frambooid diameters were not statistically different from the bone-hosted frambooid populations (sediment frambooids: $4.3 \pm 1.7 \mu\text{m}$, SD, $n = 36$, p -value = 0.1313). Frambooid microcrystal diameters were also found to be similar in size to bone-

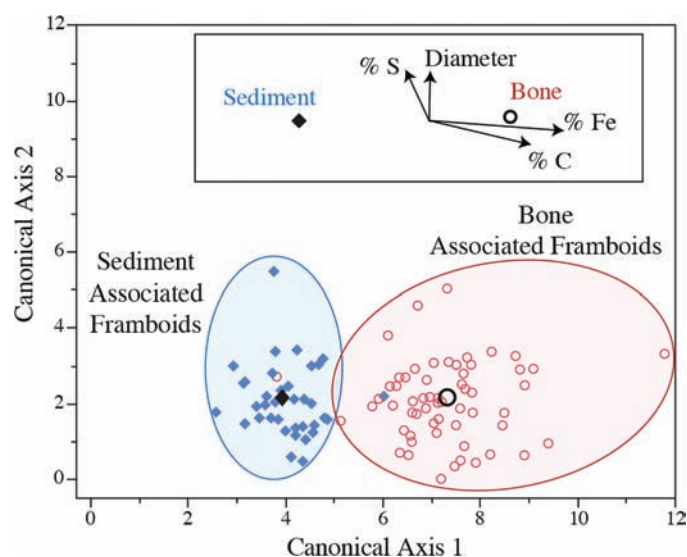


FIG. 2.—Discriminant analyses of frambooids associated with bone (open red circles) and frambooids associated with sediment (closed blue diamonds). Black symbols indicate the centroids of the sediment (diamond) and bone (open circle) populations. Ellipses indicate general frambooid populations. Axis loading plot in top right corner indicates that loading vectors of each variable, and the corresponding sediment and bone frambooid centroids, are also plotted in black symbols.

associated frambooids (sediment microcrystal diameter: $0.8 \pm 0.4 \mu\text{m}$, SD, $n = 36$, p -value = 0.1405). In contrast, elemental data do serve to distinguish sediment-hosted frambooid populations from bone-hosted populations ($p < 0.05$ for all comparisons). The mean values of bone-associated frambooids had over double the atom % Fe compared to sediment frambooids (7.9% versus 3.3%), nearly double the atom % S compared to the sediment frambooids (10.6% versus 5.8%), and also had elevated median atom % C (47.0% versus 34.2%). In addition to elemental percentages, the Fe:S ratio of the bone-hosted frambooid population was statistically higher compared to sediment frambooid population (1.3 versus 0.6). Neither of these Fe:S ratios reflect pyritic stoichiometry, but are indeed indicative of sulfide minerals in general. Sulfidic clusters were also observed in the sediment samples and were found to be statistically similar in diameter and atom % Fe, atom % S, atom % C, and Fe:S to the sediment-hosted frambooid populations ($n = 36$). As with the bone versus sediment frambooid comparisons, results from comparing the sulfidic clusters indicate that bone-hosted sulfidic clusters have similar sizes as the sediment-hosted clusters, but are distinct with respect to elemental makeup compared to the sediment-hosted clusters.

Because frambooid populations differed across many variables, we also used a multivariate approach to characterize the different frambooid populations. A discriminant analysis was performed on *a priori* groups of frambooid populations (bone and sediment) to determine the probability of frambooid group relationships based on frambooid diameter; microcrystal diameters; atom % Fe, atom % S, atom % C. Discriminant analyses generated independent linear axes that maximized separation among *a priori* groups. Group membership was then tested by cross-validation (removing a sample and re-performing discriminant group analysis). Figure 2 illustrates the discriminant analysis. Results of this analysis confirmed that frambooids from bone are distinct from sediment-associated frambooids with only a 3% cross-validation mismatch rate and significant test statistics for both the Wilks' Lambda and Pillai's Trace tests ($p < 0.001$, degrees of freedom (DF) = 6). Loading scores on each axis indicated that the elemental composition of frambooids,

primarily atom % Fe and atom % C, distinguished bone frambooids from sediment frambooids (Fig. 2).

Bone-hosted frambooids were observed to form in association with microbial biofilms at the macroscopic and microscopic level. Within the first week after bone deployment, dark microbial mats, comparable to those observed on natural or experimentally implanted whale falls (Fig. 3A), developed on bone surfaces where frambooids were also observed. By the third week of the experiment, white-colored mats developed at the peripheries of the dark mats (Fig. 3B). Under the microscope, the white mats contained filaments with a distinctive morphology comparable to *Beggiatoa* (Larkin and Strohl 1983; Nelson et al. 1989; Sassen et al. 2004) as well as other nonfilamentous bacteria housing intracellular elemental sulfur (Fig. 3C). At the microscopic level, frambooids were often found adjacent to, or encapsulated in biofilm; biofilm-associated organic matter was identified on SEM images as a feature with amorphous and homogenous texture that was distinct from bone-surface texture (Fig. 1). This material likely represents a mixture of microbial cell material and extracellular polymeric substances.

Oxygen profiles measured through the microbial mats adjacent to the bones indicate that dissolved oxygen concentrations were affected by the microbial communities in the mesocosm (Fig. 4). Before bones were introduced to the mesocosms, the water column was aerobic near the water/air interface ($\text{O}_2 > 30 \mu\text{M}$) and oxygen concentrations decreased along a gradient typical of abiotic diffusion with depth (Jørgensen and Revsbech 1985). One week after bone placement, the water column remained oxygenated, but oxygen concentrations dropped steeply at the water/microbial mat interface near the bone. Two weeks into the experiment, the water column above the bone became dysoxic ($\text{O}_2 < 30 \mu\text{M}$) while the sediment/water/biofilm interface became anoxic (no measurable O_2), even though oxygenated air was being pumped into the mesocosm (Wilkin et al. 1996) (Fig. 4). By the third week, conditions became more aerobic, with the water column becoming oxic ($\text{O}_2 > 30 \mu\text{M}$), and the pore waters moving from anoxic to dysoxic conditions. The sterilized control mesocosms showed little change in oxygen concentration throughout the experiment.

DISCUSSION

Based on elemental and discriminant analyses, as well as the location of the frambooids on the bone, we conclude that frambooids examined on bone surfaces formed *in situ* and did not originate due to resuspension of preexisting sediment frambooids. Elemental analyses of Fe, S, and C indicate that frambooid populations found on bone surfaces differ in elemental composition (atom %) from the preexisting sediment frambooid population. Bone-associated frambooids show elevated iron and carbon by over 50% compared to the sediment populations, as analyzed before and after bone placement (Fig. 1, Table 1). The separation in frambooid populations is more evident when comparing them in discriminant analyses (Fig. 2). Although discriminant analyses are designed to ensure maximum group separation, the low misclassification percentage (2%) in conjunction with significant results from group comparison tests support the conclusion that bone frambooids are different from sediment frambooids.

Observations from the lab-simulated carcass-fall experiments suggest that bone-associated frambooids formed as the result of microbial activity. Although not necessary for formation (see Ohfuji and Rickard (2005) and references therein), microbes, specifically sulfate-reducing bacteria (SRBs) are generally thought to play a role in frambooid formation (Donald and Southam 1999; Grimes et al. 2001; Popa et al. 2004; MacLean et al. 2008). Sulfate-reducing bacteria, often members of the subphylum Deltaproteobacteria, use sulfate as their terminal electron acceptor and generate sulfide as an end product. The sulfide generated by the SRBs then reacts with Fe^{2+} , to form iron monosulfide, which is a precursor to the

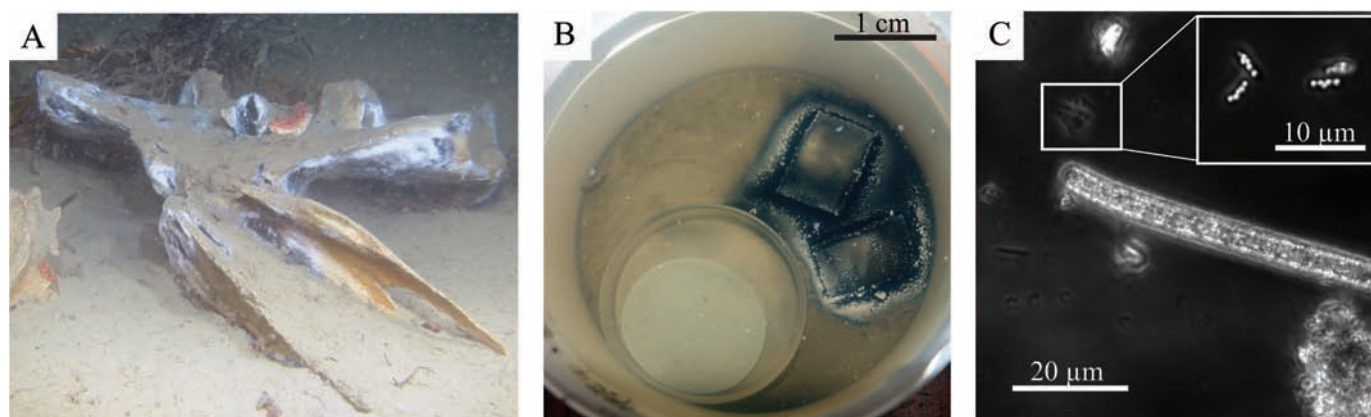


FIG. 3.—Examples of microbial mats on actual and simulated carcass falls. **A**) Image of an experimentally implanted whale fall (*Balaenoptera acutorostrata*, Minke whale) observed at 125 m depth off the coast of Sweden (referenced in Dahlgren et al. 2006). Like the mats grown in the carcass-fall simulation, cranial bones from the natural whale fall are covered in a black bacterial mat likely rich in sulfate-reducing bacteria, which in places is overlain by a white bacterial mat containing sulfide-oxidizing bacteria. Photo courtesy of Thomas Dahlgren, Adrian Glover, and Thomas Lundalv (remotely operated vehicle (ROV) pilot). **B**) Bones covered with black (sulfate-reducing) and white (sulfide-oxidizing) microbial mat after three weeks. **C**) Photomicrograph of a bone-associated microbial mat similar to those seen in carcass-fall simulations at Week 3. *Beggiatoa*, a sulfide-oxidizing filamentous bacterium, is prominent, and the inset shows smaller bacteria containing elemental sulfur (white circles).

formation of other sulfide framboids. Our observations and measurements suggest that the framboids in the carcass-fall mesocosms also formed due to sulfide produced by the microbial consortia colonizing bone. Although not directly measured in this study, the generation of sulfide due to bone emplacement in the lab-simulated carcass-fall mesocosms is indicated by the sharp decrease in oxygen concentrations near the bone biofilm (Fig. 4), the blackening of the bone surfaces and surrounding sediments (Fig. 3B), and the presence of sulfide-oxidizing bacteria (Fig. 3C). The low oxygen concentrations near the biofilms on bone surfaces indicate that the microbial community was likely living in anoxic conditions, which is favorable for the production of sulfide by sulfate-reducing bacteria. Additionally, the dark staining on bone and sediment also suggests that sulfide was generated in the mesocosm; sulfide often reacts with ambient ferrous iron and produces nanocrystallites

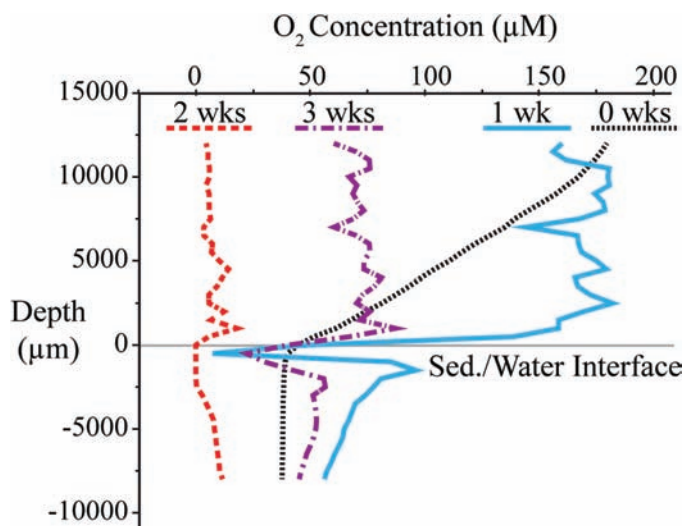


FIG. 4.—Oxygen microsensor profiles of carcass-fall mesocosms during the experiment. Despite oxygenated air being pumped into the mesocosm throughout the experiment, profiles show the progression from a typical oxygen diffusion (Week 0) to a near-anoxic water column in Week 2, and the return of dissolved oxygen in Week 3.

composed of iron monosulfide, which can stain sediment black (Canfield and Raiswell 1991; Thamdrup et al. 1994; Darroch et al. 2012; Amon et al. 2013). Under the microscope, several types of sulfide-oxidizing bacteria were identified from bone-surface biofilms including filamentous *Beggiatoa* (Fig. 3C), which are easily identified by their distinctive morphology (Larkin and Strohl 1983; Nelson et al. 1989; Sassen et al. 2004) and are known to occur in natural and experimental carcass falls as seen in Figure 3A (Deming et al. 1997; Smith and Baco 2003). Sulfide-oxidizing bacteria are often found superjacent to sulfate-reducing bacteria because they depend on the sulfide produced by the sulfate-reducing bacteria as their energy source. Thus, the presence of sulfide-oxidizing bacteria in bone biofilms indirectly supports the presence of sulfide in the mesocosm experiments. Biofilms were not observed on the mesocosm sediment before bone addition, suggesting that the microbial communities developed as a direct result of the bone, which implies that the bone organics and associated secondary metabolites fueled mat formation.

In the carcass-fall simulation, bone-hosted framboids developed on bone surfaces within one week of introducing bone to the mesocosm, suggesting that framboid formation can initiate within days in natural carcass falls occurring extremely early in the diagenetic history of fossilized remains, and substantially earlier than previously described. The decay process of natural carcass falls, especially of large marine mammals, is dynamic and long-lived, and prior to our experiment, it was unclear at which point during the decomposition history framboids would form (Kiel et al. 2008; Shapiro and Spangler 2009). Smith and Baco (2003) studied the decomposition of whale falls extensively and established four successional decomposition stages characterized by predominant scavenger types and their targeted whale tissue: (1) a mobile-scavenger stage during which most soft tissue is removed primarily by mobile scavengers; (2) an opportunist-enrichment phase composed of sessile scavengers that target organics leached into the surrounding sediment and remaining soft tissue on the bone; (3) a sulphophilic stage fueled by sulfate-reducing bacteria exploiting bone lipids, a stage that can support complex trophic assemblages; and (4) a reef stage during which nutrient-depleted bone acts as a substrate for epibionts (Smith and Baco 2003). Microbes are present and actively degrading tissue in each stage, including the initial scavenger stage, as shown by aqueous decomposition studies (Giancamillo et al. 2010). The duration of each decomposition stage is dependent on environmental conditions as well as the size, age, and taxon represented by the vertebrate

remains (Smith and Baco 2003). In general, the consumption of soft tissue and labile organics is fast and occurs within a few years, but the degradation of bone during the sulphophilic stage can be much slower, sometimes occurring over time scales of many decades (Jones et al. 1998; Smith and Baco 2003). However, the timing and duration of these stages can be highly depth dependent, and a recent time-series study by Lundsten et al. (2010) showed that not all of these stages occur in some whale falls. Whale falls in deeper water did include a sulphophilic stage, represented by thick mats of sulfide-oxidizing microbial mats similar to those observed in our experiment. However, a sulphophilic stage was not obvious in whale falls from shallower sites.

We would expect frambooids to form during the sulphophilic scavenging stage when sulfide concentrations are thought to be at their highest (Smith and Baco 2003). Indeed, a previous study used the association of sulfide frambooids, in the presence of fossil mollusks and gastropods known to harbor sulfide-utilizing symbiotic bacteria, to identify the sulphophilic scavenging stage of a fossil whale fall (Amano and Little 2005). However, since microbes were also present during the other decomposition stages, and based on the rapid formation of frambooids in our experiment, it is possible that frambooid formation is not limited to just the sulphophilic stage, and may also occur much earlier in the decomposition history. The time series studies of Lundsten et al. (2010) illustrate that while the canonical decomposition stages identified by Smith and Baco are useful for thinking about the processes occurring at whale falls in general, individual whale falls are influenced by diverse environmental factors that can result in a range of taphonomic processes and early diagenetic conditions. Our experiments indicate that sulfate-reducing bacteria colonizing bone surfaces at the very early stages of microbial decay can provide sufficient sulfide to initiate frambooid nucleation. Thus, our findings suggest that frambooid formation can occur as early as the opportunistic-enrichment phase when bones are initially exposed. Due to the limited scope of our study, we cannot confirm at which other stages of decomposition frambooids may form, although it is likely that if sulfide is being produced, even in small amounts, then frambooids have the potential to form.

Sulfate-reducing bacteria, a primary source for sulfide in the formation of frambooids, naturally exist in shallow sediment, often with their activities concentrated within localized zones of sulfate-reduction (Allison 1988). Kiel et al. (2008) have suggested that frambooids forming in association with vertebrate material likely formed when the vertebrate remains were buried at shallow depths. Our experiments also show that bones need not be buried in the zone of sulfate reduction to act as substrates for frambooid formation. Frambooids can also form on the surfaces of bone exposed at the sediment/water interface, even if the overlying water column is well oxygenated, so long as a source of reactive iron is present, as was the case in our experimental mesocosms (see Supplementary Data Table S1 for concentrations of iron in experimental sediment).

Much of the literature on frambooids focuses on their use as indicators of regional geochemical conditions (Skei 1988; Wilkin et al. 1996; Bond et al. 2004; Marynowski et al. 2007). Previous experimental and actualistic studies indicate that frambooid populations originating in euxinic conditions typical of stagnant closed basins or ocean anoxic events tend to be smaller and less variable in size compared to frambooid populations from oxygenated ocean basins (Wilkin et al. 1996; Bond et al. 2004; Marynowski et al. 2007). Frambooids from anoxic settings are thought to be smaller and less variable ($5.1 \pm 1.5 \mu\text{m SD}$) because they form in the water column and quickly sink to the seafloor after precipitation, limiting the supply of iron in a sulfide-dominated system and halting frambooid growth (Skei 1988; Wilkin et al. 1996). In comparison, frambooids that form in oxygenated water columns tend to be larger and more variable in size ($8.0 \pm 2.2 \mu\text{m SD}$) because they likely nucleate near, or at, the sediment/water interface where both iron and sulfide are available, and

the frambooids remain in conditions ideal for frambooid growth for a longer time (Wilkin et al. 1996).

To date, few if any studies have compared frambooid populations associated with vertebrate material with sedimentary frambooid populations. Although the sulfide involved in frambooid formation likely originates from the microbial decay of organic matter in both the sedimentary and carcass-fall scenarios, it is unclear if the disparity in the amount of available organics (planktonic in sedimentary systems versus large-vertebrate remains) has an impact on the size distribution of frambooid populations associated with carcass falls. Our study offers an opportunity to compare the experimental bone-hosted frambooid population where certain environmental conditions are known, with those from the literature, to determine if frambooids found in association with vertebrate material can also be used as ambient environmental indicators. Additionally, since the mechanisms responsible for governing frambooid size in sedimentary environments are relatively well known, comparisons of bone-hosted frambooids to published frambooid populations can provide additional insights into the formation and time of frambooid populations derived from bacterial decay of vertebrate remains.

When the mean frambooid diameter and corresponding standard deviation of frambooids growing on bone surfaces from this study are plotted against those from published frambooid populations originating from known environments (see table S5 for data and references), bone-associated frambooids plot closest to frambooids forming in anoxic water columns (Fig. 5). However, our microsensor measurements show an oxygenated water column in the mesocosm experiments (Fig. 4). If the water column is taken to be representative of ambient oxygen concentrations, then we might have expected the bone frambooids to plot closer to the dysoxic-oxic frambooid population. On closer inspection, measured oxygen concentrations from the carcass-fall simulations indicate that frambooids grew in localized anoxic microenvironments in the biofilm (O_2 concentrations = $0 \mu\text{M}$), despite the oxic conditions in the surrounding mesocosm water (O_2 concentrations $> 30 \mu\text{M}$). We interpret these results to indicate that larger volumes of organic matter can promote steep oxygen gradients and localized anoxic conditions that extend from the sediment/water interface to above the bone surface, even though the ambient water chemistry is oxic.

Additionally, because the bone frambooids in our mesocosm experiment are small and likely formed in the biofilm covering bone, yet plot closest to sedimentary frambooid populations that formed in suspension, we suggest that bacterially mediated anoxic and sulfidic conditions surrounding the bone were transient, likely due to nutrient availability and changing microbial communities. Subtle Eh or pH changes may abruptly stop frambooid formation; and once stopped, frambooids typically do not resume formation (Wilkin et al. 1996). Thus, we propose that the smaller frambooids that form in the microbial mat result from shorter exposure to conditions that favor frambooid growth than those that precipitate in sediment pore waters. Frambooid populations originating from the decay of vertebrate material, and possibly other transient conditions such as bacterial biofilms, may be reliable indicators of localized conditions, but not necessarily of geochemical conditions beyond their immediate microenvironment.

CONCLUSIONS

These are the first lab-based experiments to document the formation of frambooidal iron sulfide growth on vertebrate material decaying in a simulated marine setting. Analyses of individual frambooid characteristics combined with discriminant analyses support our conclusion that frambooids forming on bone are distinct authigenic precipitates. Our experiments provide a lower bound on the timing of frambooid development associated with the decay of vertebrate material. The frambooids were first discovered on bone surfaces within a week of

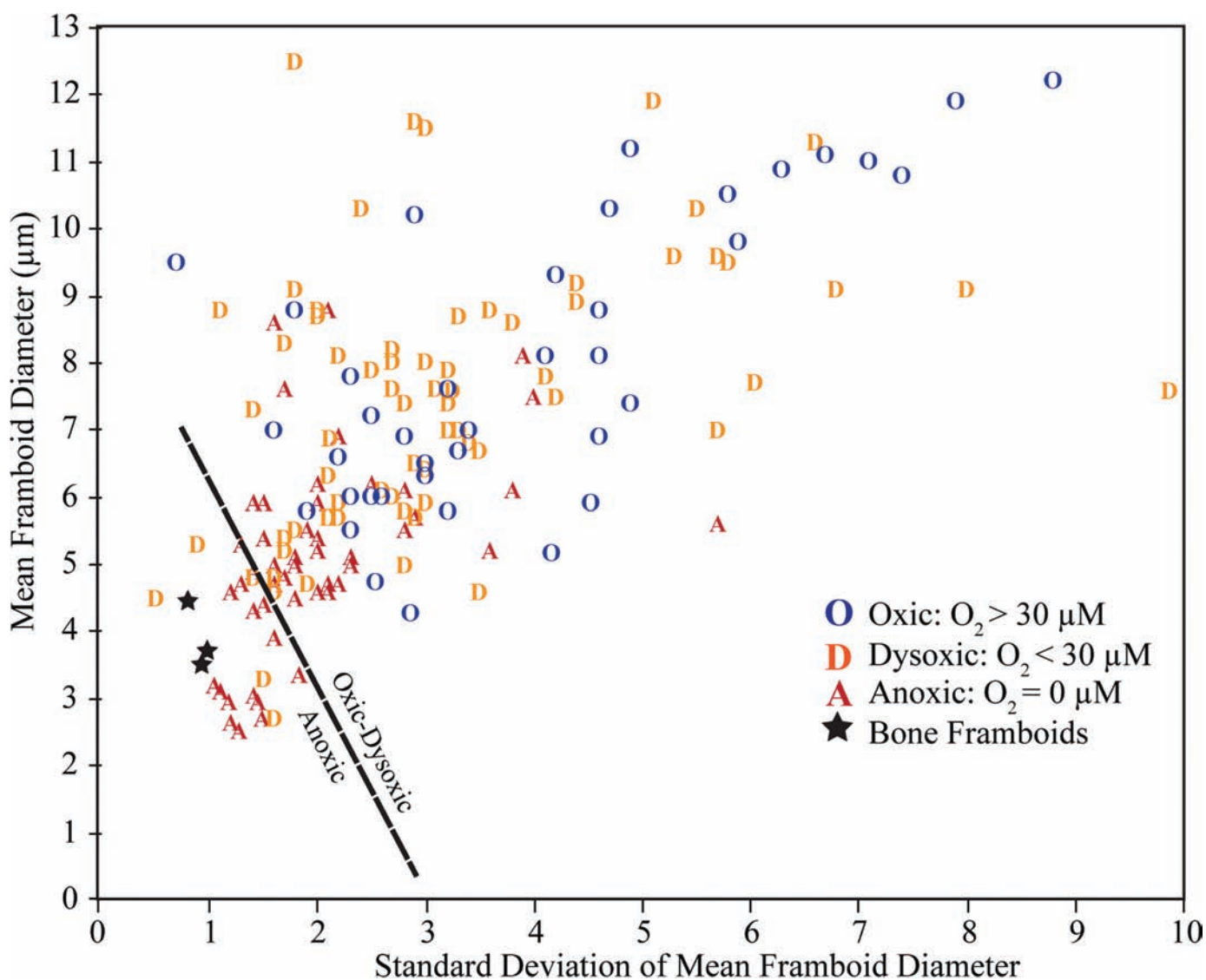


FIG. 5.—Mean frambooid diameters plotted against the standard deviation of sedimentary frambooids from known environments and from bone-hosted frambooids from this study (stars, one for each week of experimentation). Oxic-dysoxic/anoxic line is the same as identified in Wilkin et al. (2006). Values and sources for each data point are provided in Supplementary Data Table 5.

experiment initiation, and appeared in conjunction with a dark-colored microbial mat that covered bone surfaces. The black color of this microbial mat, in addition to the presence of superjacent mats of sulfide-oxidizing bacteria, suggest that sulfide was produced in the mesocosms, likely as the product of heterotrophic sulfate-reducing bacteria degrading bone organics or associated secondary metabolites. Frambooids formed as a result of localized sulfide production. Also in support of the microbial association, many frambooids on bone were found encapsulated in probable biofilm associated with the bone-covering mat. Furthermore, the direct association of frambooid appearance with the development of microbial growth on bone surfaces, coupled with the observation that frambooids did not appear in sterile control experiments, attests to the conclusion that frambooids form on bone surfaces via the indirect influences of microbial activity.

We conclude from our experiments that bones, once defleshed from scavenging, can sustain sufficient rates of sulfide production to induce frambooid precipitation early, within weeks of exposure. Our experiments show that frambooids may not necessarily indicate the sulphophilic

decomposition stage, as they may also form at the initial time of bone exposure that develops during the opportunistic-enrichment phase of large-vertebrate decay. It is possible that frambooids may develop on bone surfaces prior to soft-tissue removal and/or postburial given favorable conditions. However, we cannot comment on the likelihood of frambooids forming during these stages due to the limited duration of our experiment. Our experiments also suggest that burial is not required for frambooid formation. On comparing bone-hosted frambooid populations from the carcass-fall simulation with those from previous studies that looked at frambooid size distributions in sediments, we found that frambooids formed on vertebrate bones, or possibly in other organic loading scenarios, may not be reliable indicators of ambient oxygen concentrations in the water column, but instead represent highly localized anoxic and transient microenvironments. We found that the frambooids forming on bone surfaces under an oxic water column are similar in size to frambooid populations originating under anoxic water column conditions. We suggest that geochemical conditions associated with microbial mats developing on bone, as well as in other organic loading situations, are

dynamic, and that framboids developing in microbial mats may have shorter growing periods due to the ephemeral nature of the conditions that promote their formation on bone. Finally, because our experiments address only the initial stages of decay, more experimentation will be needed to investigate the formation of framboids at later stages of decay.

ACKNOWLEDGMENTS

We thank B. Flood and D.S. Jones for their insights into the microbial communities and geochemistry of our experiments. We also wish to thank R. Peterson from BeetleMyBones.com for providing the defleshed bones and the National Lacustrine Core Facility for their expertise and use of the SEM supported by National Science Foundation (NSF) grants 0932992 and 0652769. We thank Michael Moore for providing the marine mud and seawater. We also acknowledge the H.E. Wright Quaternary Palaeoecology Fellowship and the NSF Graduate Fellowship for support of LAV. Lastly, we acknowledge and greatly appreciate the helpful comments of two anonymous reviewers.

SUPPLEMENTAL MATERIAL

Data are available from the PALAIOS Data Archive: <http://www.sepm.org/pages.aspx?pageid=332>.

REFERENCES

- ALLISON, P.A., 1988, Taphonomy of the Eocene London clay biota: *Palaeontology*, v. 31, p. 1079–1100.
- AMANO, K., AND LITTLE, C.T., 2005, Miocene whale-fall community from Hokkaido, northern Japan: *Palaeogeography, Palaeoclimatology, Palaeoecology*, v. 215, p. 345–356.
- AMANO, K., LITTLE, C.T., AND INOUE, K., 2007, A new Miocene whale-fall community from Japan: *Palaeogeography, Palaeoclimatology, Palaeoecology*, v. 247, p. 236–242.
- AMON, D.J., GLOVER, A.G., WIKLUND, H., MARSH, L., LINSE, K., ROGERS, A.D., AND COPLEY, J.T., 2013, The discovery of a natural whale fall in the Antarctic deep sea: *Deep Sea Research Part II: Topical Studies in Oceanography*, v. 92, p. 87–96.
- BERNER, R.A., 1969, The synthesis of framboidal pyrite: *Economic Geology*, v. 64, p. 383–384.
- BERNER, R.A., 1970, Sedimentary pyrite formation: *American Journal of Science*, v. 268, p. 1–23.
- BOND, D., WIGNALL, P.B., AND RACKI, G., 2004, Extent and duration of marine anoxia during the Frasnian–Famennian (Late Devonian) mass extinction in Poland, Germany, Austria and France: *Geological Magazine*, v. 141, p. 173–193.
- BRETT, C.E., AND BAIRD, G.C., 1986, Comparative taphonomy: a key to paleoenvironmental interpretation based on fossil preservation: *PALAIOS*, v. 1, p. 207–227.
- CANFIELD, D.E., AND RAISWELL, R., 1991, Pyrite formation and fossil preservation, *in* *Taphonomy: Releasing the Data Locked in the Fossil Record*, v. 9, New York: Plenum Press, 1991, p. 337–387.
- DARROCH, S.A., LAFLAMME, M., SCHIFFBAUER, J. D., AND BRIGGS, D.E., 2012, Experimental formation of a microbial death mask: *PALAIOS*, v. 27, p. 293–303.
- DEMING, J.W., REYSENBACH, A.L., MACKO, S.A., AND SMITH, C.R., 1997, Evidence for the microbial basis of a chemoautotrophic invertebrate community at a whale fall on the deep seafloor: bone-colonizing bacteria and invertebrate endosymbionts: *Microscopy Research and Technique*, v. 37, p. 162–170.
- DONALD, R., AND SOUTHAM, G., 1999, Low temperature anaerobic bacterial diagenesis of ferrous monosulfide to pyrite: *Geochimica et Cosmochimica Acta*, v. 63, p. 2019–2023.
- FARRAND, M., 1970, Framboidal sulphides precipitated synthetically: *Mineralium Deposita*, v. 5, p. 237–247.
- GIANCAMILLO, A.D., GIUDICI, E., ANDREOLA, S., PORTA, D., GIBELLI, D., DOMENEGHINI, C., GRANDI, M., AND CATTANEO, C., 2010, Immersion of piglet carcasses in water: the applicability of microscopic analysis and limits of diatom testing on an animal model: *Legal Medicine*, v. 12, p. 13–18.
- GRIMES, S.T., BROCK, F., RICKARD, D., DAVIES, K.L., EDWARDS, D., BRIGGS, D.E., AND PARKES, R.J., 2001, Understanding fossilization: experimental pyritization of plants: *Geology*, v. 29, p. 123–126.
- GRIMES, S.T., DAVIES, K.L., BUTLER, I.B., BROCK, F., EDWARDS, D., RICKARD, D., BRIGGS, D.E., AND PARKES, R.J., 2002, Fossil plants from the Eocene London Clay: the use of pyrite textures to determine the mechanism of pyritization: *Journal of the Geological Society*, v. 159, p. 493–501.
- HOLLUND, H., JANS, M., COLLINS, M., KARS, H., JOOSTEN, I., AND KARS, S., 2012, What happened here? Bone histology as a tool in decoding the postmortem histories of archaeological bone from Castricum, The Netherlands: *International Journal of Osteoarchaeology*, v. 22, p. 537–548.
- JONES, E.G., COLLINS, M.A., BAGLEY, P.M., ADDISON, S., AND PRIEDE, I.G., 1998, The fate of cetacean carcasses in the deep sea: observations on consumption rates and succession of scavenging species in the abyssal north-east Atlantic Ocean: *Royal Society of London, Proceedings, Series B: Biological Sciences*, v. 265, p. 1119–1127.
- JØRGENSEN, B., AND REVSBECH, N., 1985, Diffusive boundary layers and the oxygen uptake of sediments and detritus: *Limnology and Oceanography*, v. 30, p. 111–122.
- KAIM, A., KOBAYASHI, Y., ECHIZENYA, H., JENKINS, R.G., AND TANABE, K., 2008, Chemosynthesis-based associations on Cretaceous plesiosaurid carcasses: *Acta Palaeontologica Polonica*, v. 53, p. 97–104.
- KASUYA, T., AND ANDO, Y., 2005, Framboidal pyrite found in a rib of the recent Balaenopteridae (Cetacea) drifted at the coast of Ibaraki Prefecture, Japan: *Japan Earth and Planetary Science Joint Meeting, Japan*, p. J030–P004.
- KIEL, S., 2008, Fossil evidence for micro- and macrofaunal utilization of large nekton-falls: examples from early Cenozoic deep-water sediments in Washington State, USA: *Palaeogeography, Palaeoclimatology, Palaeoecology*, v. 267, p. 161–174.
- LARKIN, J.M., AND STROHL, W.R., 1983, Beggiatoa, Thiolithrix, and Thioploca: *Annual Reviews in Microbiology*, v. 37, p. 341–367.
- LOVE, L., 1967, Early diagenetic iron sulphide in recent sediments of the Wash (England): *Sedimentology*, v. 9, p. 327–352.
- LUNDSTEN, L., SCHLNING, K.L., FRASIER, K., JOHNSON, S.B., KUHNZ, L.A., HARVEY, J.B., CLAGUE, G., AND VRIJENHOEK, R.C., 2010, Time-series analysis of six whale-fall communities in Monterey Canyon, California, USA: *Deep Sea Research Part I: Oceanographic Research Papers*, v. 57, p. 1573–1584.
- MACLEAN, L., TYLISZCZAK, T., GILBERT, P., ZHOU, D., PRAY, T., ONSTOTT, T., AND SOUTHAM, G., 2008, A high-resolution chemical and structural study of framboidal pyrite formed within a low-temperature bacterial biofilm: *Geobiology*, v. 6, p. 471–480.
- MARTILL, D.M., 1987, A taphonomic and diagenetic case study of a partially articulated ichthyosaur: *Palaeontology*, v. 30, p. 543–555.
- MARYNOWSKI, L., RAKOCINSKI, M., AND ZATON, M., 2007, Middle Famennian (Late Devonian) interval with pyritized fauna from the Holy Cross Mountains (Poland): organic geochemistry and pyrite framboid diameter study: *Geochemical Journal*, v. 41, p. 187–200.
- NAGANUMA, T., WADA, H., AND FUJIOKA, K., 1996, Biological community and sediment fatty acids associated with the deep-sea whale skeleton at the Torishima Seamount: *Journal of Oceanography*, v. 52, p. 1–15.
- NELSON, D.C., WIRSEN, C.O., AND JANNASCH, H.W., 1989, Characterization of large, autotrophic Beggiatoa spp. abundant at hydrothermal vents of the Guaymas Basin: *Applied and Environmental Microbiology*, v. 55, p. 2909–2917.
- OHFUJI, H., AND RICKARD, D., 2005, Experimental syntheses of framboids: a review: *Earth-Science Reviews*, v. 71, p. 147–170.
- POPA, R., KINKLE, B.K., AND BADESCU, A., 2004, Pyrite framboids as biomarkers for iron-sulfur systems: *Geomicrobiology Journal*, v. 21, p. 193–206.
- PYENSON, N.D., IRMIS, R.B., LIPPS, J.H., BARNES, L.G., MITCHELL, E.D., AND McLEOD, S.A., 2009, Origin of a widespread marine bonebed deposited during the middle Miocene Climatic Optimum: *Geology*, v. 37, p. 519–522.
- RAISWELL, R., 1982, Pyrite texture, isotopic composition and the availability of iron: *American Journal of Science*, v. 282, p. 1244–1263.
- RAISWELL, R., WHALER, K., DEAN, S., COLEMAN, M., AND BRIGGS, D., 1993, A simple three-dimensional model of diffusion-with-precipitation applied to localised pyrite formation in framboids, fossils and detrital iron minerals: *Marine Geology*, v. 113, p. 89–100.
- REVSBECH, N.P., 1989, An oxygen microsensor with a guard cathode: *Limnology and Oceanography*, v. 34, p. 474–478.
- REVSBECH, N.P., AND JØRGENSEN, B., 1986, Microelectrodes: their use in microbial ecology: *Advances in Microbial Ecology*, v. 9, p. 293–352.
- SASSEN, R., ROBERTS, H.H., CARNEY, R., MILKOV, A.V., DEFREITAS, D.A., LANOIL, B., AND ZHANG, C., 2004, Free hydrocarbon gas, gas hydrate, and authigenic minerals in chemosynthetic communities of the northern Gulf of Mexico continental slope: relation to microbial processes: *Chemical Geology*, v. 205, p. 195–217.
- SHAPIRO, R.S., AND SPANGLER, E., 2009, Bacterial fossil record in whale-falls: petrographic evidence of microbial sulfate reduction: *Palaeogeography, Palaeoclimatology, Palaeoecology*, v. 274, p. 196–203.
- SKEL, J., 1988, Formation of framboidal iron sulfide in the water of a permanently anoxic fjord: Framvaren, South Norway: *Marine Chemistry*, v. 23, p. 345–352.
- SMITH, C.R., AND BACO, A.R., 2003, Ecology of whale falls at the deep-sea floor: *Oceanography and Marine Biology: An Annual Review Volume*, v. 41, p. 311–354.
- SWEENEY, R., AND KAPLAN, I., 1973, Pyrite framboid formation; laboratory synthesis and marine sediments: *Economic Geology*, v. 68, p. 618–634.
- THAMDRUP, B., FOSSING, H., AND JØRGENSEN, B.B., 1994, Manganese, iron and sulfur cycling in a coastal marine sediment, Aarhus Bay, Denmark: *Geochimica et Cosmochimica Acta*, v. 58, p. 5115–5129.
- TURNER-WALKER, G., 2012, Early bioerosion in skeletal tissues: persistence through deep time: *Neues Jahrbuch für Geologie und Paläontologie-Abhandlungen*, v. 265, p. 165–183.
- TURNER-WALKER, G., AND JANS, M., 2008, Reconstructing taphonomic histories using histological analysis: *Palaeogeography, Palaeoclimatology, Palaeoecology*, v. 266, p. 227–235.
- WILKIN, R., BARNES, H., AND BRANTLEY, S., 1996, The size distribution of framboidal pyrite in modern sediments: an indicator of redox conditions: *Geochimica et Cosmochimica Acta*, v. 60, p. 3897–3912.
- ZHOU, C., AND JIANG, S.-Y., 2009, Palaeoceanographic redox environments for the lower Cambrian Hetang Formation in South China: evidence from pyrite framboids, redox sensitive trace elements, and sponge biota occurrence: *Palaeogeography, Palaeoclimatology, Palaeoecology*, v. 271, p. 279–286.

Received 14 March 2014; accepted 16 January 2015.